Bull. Nov. Comp. Center, Math. Model. in Geoph., 12 (2008), 1–14

Modeling of wave fields for various structures of mud volcanoes*

B.M. Glinsky, D.A. Karavaev, V.V. Kovalevsky, V.N. Martynov

In the Kerch–Tamagne areas, mud volcanoes and associated "pressed synclines" are evolving. The problem of genesis of mud volcanoes is debated; researchers of mud volcanoes do not have a common opinion about the mechanism of their formation. The necessity of studying the mud volcanoes structures is also connected with the fact that some mud volcanoes in the Tamagne mud volcanoes provinces represent a real danger for the population at moments of intensive eruptions because of the immediate proximity from settlements.

It is not excluded that processes associated with general decontamination of the Earth underlies the mechanism of formation of mud volcanoes. It is known that millions of cubic meters of methane per day are derived from the Black sea bottom.

In [1–5], the proposed vibroseismic method of monitoring the magmatic structures with a controllable seismic source will make possible to receive a new knowledge about the structure of volcanoes, their origin and dynamics of the behavior of dilatancy structures of living volcanoes with vibroseismic monitoring of these structures.

The solution to the fundamental problem of studying the structures of mud volcanoes is related to the development of theoretical, methodical and experimental bases of sounding the dilatancy zones of volcanoes with application of powerful vibrators. One of the key problems of studying volcanoes of the given type is the construction an adequate mathematical models for given structures describing the propagation of elastic waves generated by a powerful vibrator.

It is known that mathematical modeling is an effective tool to study the processes of propagation of elastic waves in various models of complex subsurface geometries. Currently, a wide spectrum of numerical methods as applied to the full wave fields simulation in inhomogeneous elastic media is available, for example [6]. The difference method and the finite element method are the most flexible from all known methods of numerical modeling of elastic waves propagation in the case of complicated three-dimensional

*Supported by Russian Foundation for Basic Research under Grants 05-05-64245, 06-05-65265, 04-05-64177, 07-05-00858, 07-07-00214; programs of the RFBR No. 16.12, 16.13, 16.15; and Interdisciplinary Integration Project of SB RAS No. 16.57.

inhomogeneous elastic media. However, their use demands high computer costs even with application of the cluster super computers.

The developed program is intended for the numerical modeling of elastic waves propagation in three-dimensional inhomogeneous models of elastic media, using a finite difference method.

In 1], the results of the first vibroseismic experiments of research into the mud volcano Shugo are presented. It was found out that the wave field of seismic waves has a complex structure in the volcano vicinity. Further direction of experimental research will be defined by the results of numerical modeling to be used when interpreting the data of vibroseismic sounding of mud volcanoes in the Tamagne province.

We propose the further investigation of volcanic pipes using vibroseismic methods with application of seismic vibrators and areal recording systems. It is assumed that the choice of the scheme of observation and interpretation of results of field experiments will be made on the basis of results of mathematical modeling.

1. Statement of problem

Numerical modeling of processes of the seismic waves propagation in complex subsurface geometries is carried out on the basis of a full system of equations of elasticity theory written down in velocities of displacements and stresses.

For calculation of theoretical seismograms resulting from the influence of a concentrated source located in an anisotropic medium it is necessary to define components of the vector of displacement velocities (U, V, W) and the strain tensor $(\sigma_{xx}, \sigma_{yy}, \sigma_{zz}, \sigma_{xy}, \sigma_{xz}, \sigma_{yz})$, satisfying the following equations:

$$
\begin{aligned}
\rho\frac{\partial U}{\partial t} &= \frac{\partial \sigma_{xx}}{\partial x} + \frac{\partial \sigma_{xy}}{\partial y} + \frac{\partial \sigma_{xz}}{\partial z} + F_x(t,x,y,z),\\
\rho\frac{\partial V}{\partial t} &= \frac{\partial \sigma_{xy}}{\partial x} + \frac{\partial \sigma_{yy}}{\partial y} + \frac{\partial \sigma_{yz}}{\partial z} + F_y(t,x,y,z),\\
\rho\frac{\partial W}{\partial t} &= \frac{\partial \sigma_{xz}}{\partial x} + \frac{\partial \sigma_{yz}}{\partial y} + \frac{\partial \sigma_{zz}}{\partial z} + F_z(t,x,y,z),\\
\frac{\partial \sigma_{xx}}{\partial t} &= (\lambda+2\mu)\frac{\partial U}{\partial x} + \lambda\frac{\partial V}{\partial y} + \lambda\frac{\partial W}{\partial z},\\
\frac{\partial \sigma_{yy}}{\partial t} &= \lambda\frac{\partial U}{\partial x} + (\lambda+2\mu)\frac{\partial V}{\partial y} + \lambda\frac{\partial W}{\partial z},\\
\frac{\partial \sigma_{zz}}{\partial t} &= \lambda\frac{\partial U}{\partial x} + \lambda\frac{\partial V}{\partial y} + (\lambda+2\mu)\frac{\partial W}{\partial z},\\
\frac{\partial \sigma_{xz}}{\partial t} &= \mu\left(\frac{\partial U}{\partial z} + \frac{\partial W}{\partial x}\right),
\end{aligned}
$$

$$\frac{\partial \sigma_{yz}}{\partial t} = \mu\left(\frac{\partial V}{\partial z} + \frac{\partial W}{\partial y}\right),$$
$$\frac{\partial \sigma_{xy}}{\partial t} = \mu\left(\frac{\partial U}{\partial y} + \frac{\partial V}{\partial x}\right)$$

with the initial conditions

$$U(x,y,z,t)\big|_{t=0} = V(x,y,z,t)\big|_{t=0} = W(x,y,z,t)\big|_{t=0} = 0$$

and the boundary conditions

$$\sigma_{xz}\big|_{z=0} = \sigma_{yz}\big|_{z=0} = \sigma_{zz}\big|_{z=0} = 0.$$

The density $\rho = \rho(x,y,z)$ is supposed to depend on the coordinate x, y, and z, and the right-hand side has the following form:

$$\vec{F}(t,x,y,z) = F_x\vec{i} + F_y\vec{j} + F_z\vec{k}.$$

For example, for a source of the type "vertical force" type we have:

$$\vec{F}(t,x,y,z) = \delta(x-x_0)\delta(y-y_0)\delta(z-z_0)f(t)\vec{k},$$

where (x_0, y_0, z_0) are the coordinates of the source.

2. Method of solution

The technique of a problem solution is based on the finite difference method. The principles of constructing a difference scheme is based on the method of finite volumes considered in [7]. The basic condition of constructing the scheme used is the fulfilment of integral laws of conservation.

In this connection, the difference factors (λ, $\lambda + 2\mu$, μ, ρ which can have discontinuities) that participate in a difference scheme are calculated on the basis of integral laws of conservation [7].

For this purpose, we convert the Hooke matrix. The new values approximating the integrated law of conservation are recalculated with the formulas presented in [7], then we convert the matrix again and obtain the one with factors to be used to resolve the scheme.

The resulting scheme has the second order of approximation with respect to time and space [7].

The general version of the finite difference scheme is implemented for grids with a variable step, but for simplicity, a version of the scheme with equal steps in spatial variables is considered here.

The finite difference scheme in this case is as follows:

$$\frac{\rho_{ijk}+\rho_{i-1jk}}{2}\frac{u^{n+1}_{i-\frac{1}{2}jk}-u^{n}_{i-\frac{1}{2}jk}}{\tau}=\frac{\sigma^{n+\frac{1}{2}}_{xxijk}-\sigma^{n+\frac{1}{2}}_{xxi-1jk}}{\Delta x}+$$
$$\frac{\sigma^{n+\frac{1}{2}}_{xyi-\frac{1}{2}j+\frac{1}{2}k}-\sigma^{n+\frac{1}{2}}_{xyi-\frac{1}{2}j-\frac{1}{2}k}}{\Delta y}+\frac{\sigma^{n+\frac{1}{2}}_{xzi-\frac{1}{2}jk+\frac{1}{2}}-\sigma^{n+\frac{1}{2}}_{xzi-\frac{1}{2}jk-\frac{1}{2}}}{\Delta z}+f^{n}_{xijk},$$
$$\frac{\rho_{ijk}+\rho_{ij-1k}}{2}\frac{v^{n+1}_{ij-\frac{1}{2}k}-v^{n}_{ij-\frac{1}{2}k}}{\tau}=\frac{\sigma^{n+\frac{1}{2}}_{xyi+\frac{1}{2}j-\frac{1}{2}k}-\sigma^{n+\frac{1}{2}}_{xyi-\frac{1}{2}j-\frac{1}{2}k}}{\Delta x}+$$
$$\frac{\sigma^{n+\frac{1}{2}}_{yyijk}-\sigma^{n+\frac{1}{2}}_{yyij-1k}}{\Delta y}+\frac{\sigma^{n+\frac{1}{2}}_{yzij-\frac{1}{2}k+\frac{1}{2}}-\sigma^{n+\frac{1}{2}}_{yzij-\frac{1}{2}k-\frac{1}{2}}}{\Delta z}+f^{n}_{yijk},$$
$$\frac{\rho_{ijk}+\rho_{ijk-1}}{2}\frac{w^{n+1}_{ijk-\frac{1}{2}}-w^{n}_{ijk-\frac{1}{2}}}{\tau}=\frac{\sigma^{n+\frac{1}{2}}_{xzi+\frac{1}{2}jk-\frac{1}{2}}-\sigma^{n+\frac{1}{2}}_{xzi-\frac{1}{2}jk-\frac{1}{2}}}{\Delta x}+$$
$$\frac{\sigma^{n+\frac{1}{2}}_{yzij+\frac{1}{2}k-\frac{1}{2}}-\sigma^{n+\frac{1}{2}}_{yzij-\frac{1}{2}k-\frac{1}{2}}}{\Delta y}+\frac{\sigma^{n+\frac{1}{2}}_{zzijk}-\sigma^{n+\frac{1}{2}}_{zzijk-1}}{\Delta z}+f^{n}_{zijk},$$
$$\frac{\sigma^{n+\frac{1}{2}}_{xxijk}-\sigma^{n-\frac{1}{2}}_{xxijk}}{\tau}=(\lambda+2\mu)_{ijk}\frac{u^{n}_{i+\frac{1}{2}jk}-u^{n}_{i-\frac{1}{2}jk}}{\Delta x}+$$
$$\lambda_{ijk}\frac{v^{n}_{ij+\frac{1}{2}k}-v^{n}_{ij-\frac{1}{2}k}}{\Delta y}+\lambda_{ijk}\frac{w^{n}_{ijk+\frac{1}{2}}-w^{n}_{ijk-\frac{1}{2}}}{\Delta z},\qquad(1)$$
$$\frac{\sigma^{n+\frac{1}{2}}_{yyijk}-\sigma^{n-\frac{1}{2}}_{yyijk}}{\tau}=\lambda_{ijk}\frac{u^{n}_{i+\frac{1}{2}jk}-u^{n}_{i-\frac{1}{2}jk}}{\Delta x}+$$
$$(\lambda+2\mu)_{ijk}\frac{v^{n}_{ij+\frac{1}{2}k}-v^{n}_{ij-\frac{1}{2}k}}{\Delta y}+\lambda_{ijk}\frac{w^{n}_{ijk+\frac{1}{2}}-w^{n}_{ijk-\frac{1}{2}}}{\Delta z},$$
$$\frac{\sigma^{n+\frac{1}{2}}_{zzijk}-\sigma^{n-\frac{1}{2}}_{zzijk}}{\tau}=\lambda_{ijk}\frac{u^{n}_{i+\frac{1}{2}jk}-u^{n}_{i-\frac{1}{2}jk}}{\Delta x}+$$
$$\lambda_{ijk}\frac{v^{n}_{ij+\frac{1}{2}k}-v^{n}_{ij-\frac{1}{2}k}}{\Delta y}+(\lambda+2\mu)_{ijk}\frac{w^{n}_{ijk+\frac{1}{2}}-w^{n}_{ijk-\frac{1}{2}}}{\Delta z},$$
$$\frac{\sigma^{n+\frac{1}{2}}_{xzi-\frac{1}{2}jk-\frac{1}{2}}-\sigma^{n-\frac{1}{2}}_{xzi-\frac{1}{2}jk-\frac{1}{2}}}{\tau}=$$
$$c44_{i-\frac{1}{2}jk-\frac{1}{2}}\left(\frac{u^{n}_{i-\frac{1}{2}jk}-u^{n}_{i-\frac{1}{2}jk-1}}{\Delta z}+\frac{w^{n}_{ijk-\frac{1}{2}}-w^{n}_{i-1jk-\frac{1}{2}}}{\Delta x}\right),$$
$$\frac{\sigma^{n+\frac{1}{2}}_{yzij-\frac{1}{2}k-\frac{1}{2}}-\sigma^{n-\frac{1}{2}}_{yzij-\frac{1}{2}k-\frac{1}{2}}}{\tau}=$$
$$c55_{ij-\frac{1}{2}k-\frac{1}{2}}\left(\frac{v^{n}_{ij-\frac{1}{2}k}-v^{n}_{ij-\frac{1}{2}k-1}}{\Delta z}+\frac{w^{n}_{ijk-\frac{1}{2}}-w^{n}_{ij-1k-\frac{1}{2}}}{\Delta y}\right),$$

$$\frac{\sigma^{n+\frac{1}{2}}_{xyi-\frac{1}{2}j-\frac{1}{2}k} - \sigma^{n-\frac{1}{2}}_{xyi-\frac{1}{2}j-\frac{1}{2}k}}{\tau} =$$
$$c66_{i-\frac{1}{2}j-\frac{1}{2}k}\left(\frac{u^n_{i-\frac{1}{2}jk} - u^n_{i-\frac{1}{2}j-1k}}{\Delta y} + \frac{v^n_{ij-\frac{1}{2}k} - v^n_{i-1j-\frac{1}{2}k}}{\Delta x}\right).$$

An example of calculation of the weighed factor $c66$ for calculation of σ_{xy} is as follows:

$$c66_{i-\frac{1}{2}j-\frac{1}{2}k} = 4\left(\frac{1}{\mu_{ijk}} + \frac{1}{\mu_{i-1jk}} + \frac{1}{\mu_{ij-1k}} + \frac{1}{\mu_{i-1j-1k}}\right)^{-1}.$$

Factors $c55$ and $c44$ are defined by similar formulas.

We have the following criterion of stability of the scheme in question [7]:

$$\tau \leq \frac{1}{V_{p,\max}\sqrt{\frac{1}{\Delta x^{\frac{1}{2}}} + \frac{1}{\Delta y^{\frac{1}{2}}} + \frac{1}{\Delta z^{\frac{1}{2}}}}}.$$

Here Δx, Δy, Δz are discretization steps in spatial variables and τ is a discretization step with respect to time; $V_{p,\max}$ is a maximal velocity of elastic waves propagation.

The general scheme of calculations looks as follows. First, at the first time half-step, components of the vector of displacement velocity and then at the second time half-step, necessary stress components are defined. Further, the new components of the vector of displacement velocity are calculated on a new time half-step.

3. The method of absorbing boundaries

It is necessary to use absorbing boundaries because the calculation domain is limited. The absorbing boundaries are necessary when we want no reflections of elastic waves from boundaries of the calculation domain. In this paper, we use the realization of the PML ("Perfectly Matched Layers") method idea that is stated in [8, 9].

The essence of a method is in creating an absorbing zone. In such a zone, the basic desired values are recalculated with finite difference formulas (2), and outside of the absorbing zone all is recalculated with initial finite difference scheme (1).

To describe the PML method let us construct a finite difference scheme for discretization of equations in the absorbing zone. For simplicity, let us present equations of the finite difference scheme, the other equations being obtained in a similar way. Before we turn directly to the equations for calculation of the absorbing boundaries, let us introduce the following notations:

$$
\begin{aligned}
u &= u^x + u^y + u^z, & \sigma_{xx} &= \sigma^x_{xx} + \sigma^y_{xx} + \sigma^z_{xx}, & \sigma_{xy} &= \sigma^x_{xy} + \sigma^y_{xy},\\
v &= v^x + v^y + v^z, & \sigma_{yy} &= \sigma^x_{yy} + \sigma^y_{yy} + \sigma^z_{yy}, & \sigma_{xz} &= \sigma^x_{xz} + \sigma^z_{xz},\\
w &= w^x + w^y + w^z, & \sigma_{zz} &= \sigma^x_{zz} + \sigma^y_{zz} + \sigma^z_{zz}, & \sigma_{yz} &= \sigma^y_{yz} + \sigma^z_{yz}.
\end{aligned}
$$

Thus, each of the desired values is represented as sum of several components, whose values should be defined. Then, applying the method [8], the equations for calculation in the absorbing zone will take the form:

$$
\begin{aligned}
&\rho = \frac{\rho_{ijk} + \rho_{i-1jk}}{\frac{1}{2}},\\
&\rho\left(\frac{u^{x\,n+1}_{i-\frac{1}{2}jk} - u^{x\,n}_{i-\frac{1}{2}jk}}{\tau} + d^x\frac{u^{x\,n+1}_{i-\frac{1}{2}jk} - u^{x\,n}_{i-\frac{1}{2}jk}}{2}\right) = \frac{\sigma^{n+\frac{1}{2}}_{xxijk} - \sigma^{n+\frac{1}{2}}_{xxi-1jk}}{\Delta x} + f_{xijk},\\
&\rho\left(\frac{u^{y\,n+1}_{i-\frac{1}{2}jk} - u^{y\,n}_{i-\frac{1}{2}jk}}{\tau} + d^y\frac{u^{y\,n+1}_{i-\frac{1}{2}jk} - u^{y\,n}_{i-\frac{1}{2}jk}}{2}\right) = \frac{\sigma^{n+\frac{1}{2}}_{xyi-\frac{1}{2}j+\frac{1}{2}k} - \sigma^{n+\frac{1}{2}}_{xyi-\frac{1}{2}j-\frac{1}{2}k}}{\Delta y},\\
&\rho\left(\frac{u^{z\,n+1}_{i-\frac{1}{2}jk} - u^{z\,n}_{i-\frac{1}{2}jk}}{\tau} + d^z\frac{u^{z\,n+1}_{i-\frac{1}{2}jk} - u^{z\,n}_{i-\frac{1}{2}jk}}{2}\right) = \frac{\sigma^{n+\frac{1}{2}}_{xzi-\frac{1}{2}jk+\frac{1}{2}} - \sigma^{n+\frac{1}{2}}_{xzi-\frac{1}{2}jk-\frac{1}{2}}}{\Delta z},\\
&\frac{\sigma^{x\,n+\frac{1}{2}}_{xxijk} - \sigma^{x\,n-\frac{1}{2}}_{xxijk}}{\tau} + d^x\frac{\sigma^{x\,n+\frac{1}{2}}_{xxijk} - \sigma^{x\,n-\frac{1}{2}}_{xxijk}}{2} = (\lambda+2\mu)_{ijk}\frac{u^n_{i+\frac{1}{2}jk} - u^n_{i-\frac{1}{2}jk}}{\Delta x},\\
&\frac{\sigma^{y\,n+\frac{1}{2}}_{xxijk} - \sigma^{y\,n-\frac{1}{2}}_{xxijk}}{\tau} + d^y\frac{\sigma^{y\,n+\frac{1}{2}}_{xxijk} - \sigma^{y\,n-\frac{1}{2}}_{xxijk}}{2} = \lambda_{ijk}\frac{v^n_{ij+\frac{1}{2}k} - v^n_{ij-\frac{1}{2}k}}{\Delta y},\\
&\frac{\sigma^{z\,n+\frac{1}{2}}_{xxijk} - \sigma^{z\,n-\frac{1}{2}}_{xxijk}}{\tau} + d^z\frac{\sigma^{z\,n+\frac{1}{2}}_{xxijk} - \sigma^{z\,n-\frac{1}{2}}_{xxijk}}{2} = \lambda_{ijk}\frac{w^n_{ijk+\frac{1}{2}} - w^n_{ijk-\frac{1}{2}}}{\Delta z},\\
&\frac{\sigma^{x\,n+\frac{1}{2}}_{xyi-\frac{1}{2}j-\frac{1}{2}k} - \sigma^{x\,n-\frac{1}{2}}_{xyi-\frac{1}{2}j-\frac{1}{2}k}}{\tau} + d^x\frac{\sigma^{x\,n+\frac{1}{2}}_{xyi-\frac{1}{2}j-\frac{1}{2}k} - \sigma^{x\,n-\frac{1}{2}}_{xyi-\frac{1}{2}j-\frac{1}{2}k}}{2} =\\
&\qquad c66_{i-\frac{1}{2}j-\frac{1}{2}k}\frac{u^n_{i-\frac{1}{2}jk} - u^n_{i-\frac{1}{2}j-1k}}{\Delta y},\\
&\frac{\sigma^{y\,n+\frac{1}{2}}_{xyi-\frac{1}{2}j-\frac{1}{2}k} - \sigma^{y\,n-\frac{1}{2}}_{xyi-\frac{1}{2}j-\frac{1}{2}k}}{\tau} + d^y\frac{\sigma^{y\,n+\frac{1}{2}}_{xyi-\frac{1}{2}j-\frac{1}{2}k} - \sigma^{y\,n-\frac{1}{2}}_{xyi-\frac{1}{2}j-\frac{1}{2}k}}{2} =\\
&\qquad C66_{i-\frac{1}{2}j-\frac{1}{2}k}\frac{v^n_{ij-\frac{1}{2}k} - v^n_{i-1j-\frac{1}{2}k}}{\Delta x}.
\end{aligned}
\tag{2}
$$

Here d^x, d^y, d^z are factors of absorption along the corresponding directions of spatial variables. The presented equations correspond to the PML model in the nodes, where absorption in all three directions is required. The calculation inside the PML layers is done with zero factor of absorption in the direction that is orthogonal to that of calculation. Let us consider this on an example of the cross-section in plane Oxy: $d^x = 0$ for the PML

layers along the direction y and $d^y = 0$ for the PML layers along the direction x. Having defined the components u^x, u^y, u^z from the equations, we obtain the final value of u by summation of all the defined components $u = u^x + u^y + u^z$ for each point of the finite difference scheme in the PML zone. In the same manner, we obtain the value $\sigma_{xx} = \sigma^x_{xx} + \sigma^y_{xx} + \sigma^z_{xx}$ for the PML domain. Similar operations take place for the rest finite difference equations for obtaining the desired values in absorption zones.

4. Construction of three-dimensional model of elastic media

The problem of constructing a three-dimensional model of an elastic medium is sufficiently complicated. There are several ways of assigning a three-dimensional model of the elastic media.

In the general case, it is supposed that the three-dimensional model of media (λ, μ, ρ) is set in the nodes of a three-dimensional grid with arbitrary steps in spatial variables. In this case, it is assumed that any external "constructor" of model is used.

We used the own constructor of the model realizing the construction of a tree-dimensional model of elastic media to carry out the calculations needed here.

Let there be built a coarse-grain model of a medium. This model consists of parallelepipeds, in whose vertices parameters of this medium are set. The parameters are continuous inside each block, the discontinuity of the media parameters on the boundaries of blocks being allowed. Then there is an interpolation of necessary values (parameters of the medium) onto a finer grid with help of a finite element method. Then geometrical objects (which are analytically set): cylindrical, conic, ellipsoidal, etc., can be imbedded into a constructed 3D medium model on the fine-grain grid. Such objects can substitute the parameters on this fine with their own parameters. We allow the possibility of intersection and imbedding of objects. Thus, the medium parameters are defined by objects according to the given priority [10].

As a result, the "constructor" of elastic media model defines data needed for calculation of the factors λ, μ, $\lambda + 2\mu$, and ρ at each point of a difference scheme.

The developed "constructor" of the model makes possible to set complicated models of media that are close to real objects.

5. Algorithm of program parallelization

There are two realizations of a parallel program with the help of the parallel programming languages MPI and OpenMP. In view of the tendency of development of the multiprocessor cluster systems, where the majority of clusters consist of "nodes", which include several multicore processors with common

memory, it is meaningful to apply a "hybrid" technology of parallelization for the three-dimensional finite difference schemes. We will use OpenMP for parallelization inside each "node", and MPI between "nodes". This considerably reduces the volume of information exchanges between the nodes. Subdivision of the calculation domain into layers along the coordinate Z is technologically convenient for both versions. The number of nodes in each layer is defined depending on the number of possible computing cores. Each computing node will calculate the number of layers equal to that of processor cores it has. For data exchange in a boundary layers nodes the MPI version of a parallel program is used.

6. Models for numerical calculations

Results of field experiments have shown that the structure of mud volcanoes has a complex geometry and an inhomogeneous structure of a medium, which contains a liquid, bubbles of gas, non- inhomogeneous inclusions, etc. All this have an influence on the structure of a wave field observable in the experiments. In this paper, we carry out numerical modeling, for presenting influence of geometry of a model on the structure of a wave field. This means we do not consider the features connected with the presence of a heterogeneous media structure. In this case, at the first stage, we consider simple models, which allow studying the main features.

To study the structure of wave field obtained when carrying out field experiments with the mud volcanoes in the Kerch–Tamagne area, test calculations were done for the following models of media.

In all models under study, the medium consists of three horizontal layers (a middle layer is low-velocity and has thickness of 1 km). A cylindrical subarea with elastic properties similar to those of the middle layer is imbedded into the upper layer. The coordinates of the center of the base of cylinder are (4.4 km, 3.5 km).

The containing medium has the following parameters: $V_p = 2$ km/s, $V_s = 1$ km/s, $\rho = 1$ g/sm^3. The cylindrical subarea and the middle layer have the parameters $V_p = 1$ km/s, $V_s = 0.7$ km/s, $\rho = 1$ g/sm^3.

Figures 1–4 present the models under study: the cross-section with the plane Oxz of the domain in question which passes through the center of a source, and with the plane Oxy near to the free surface. The size of the containing medium being 7 km in all directions.

The source of "the center of pressure" type with a carrier frequency of 4 Hz is close to the free surface. The coordinates of the source are (3 km, 3.5 km, 0.4 km).

Four sensor cables of observation are located near to the free surface, each one containing 25 geophones. A distance between the geophones is 0.25 km. The places of sensors are marked with numbers on Figures 1–4.

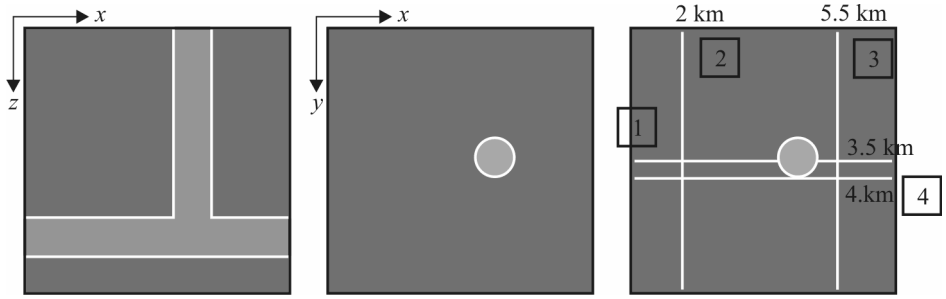

Figure 1. Model 1: The base of cylinder is a circle of 1 km diameter

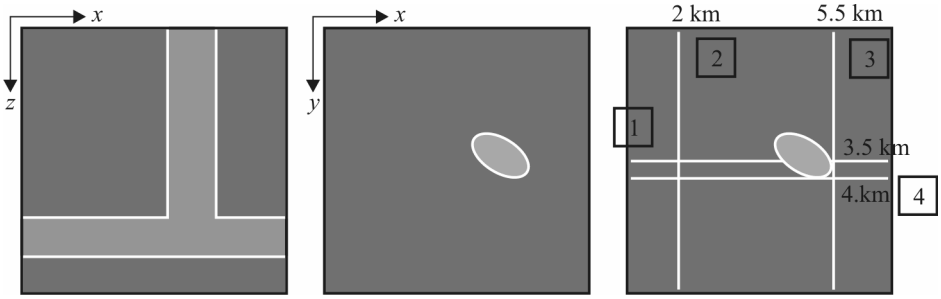

Figure 2. Model 2: The base of cylinder is an ellipse with semi-axes of 0.8 and 0.4 km

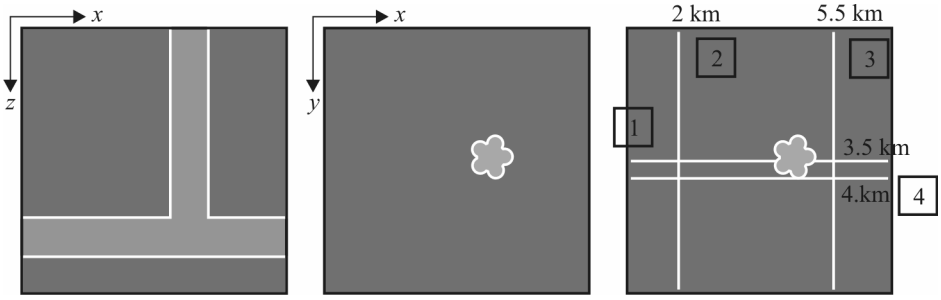

Figure 3. Model 3: The base of cylinder is a shape composed from circles of 0.2 km diameter

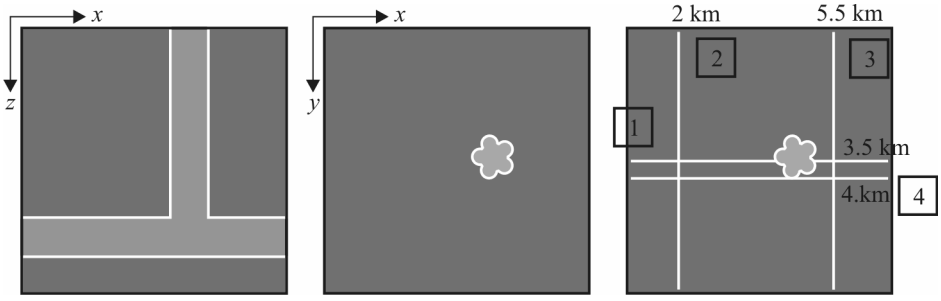

Figure 4. Model 4: The base of cylinder is a shape composed from circles of 0.2 km diameter

7. Results of numerical modeling

In Figures 5–12, the snapshots of a wave field were made in the planes Oxy, Oxz, and Oyz passing through the point of the source location.

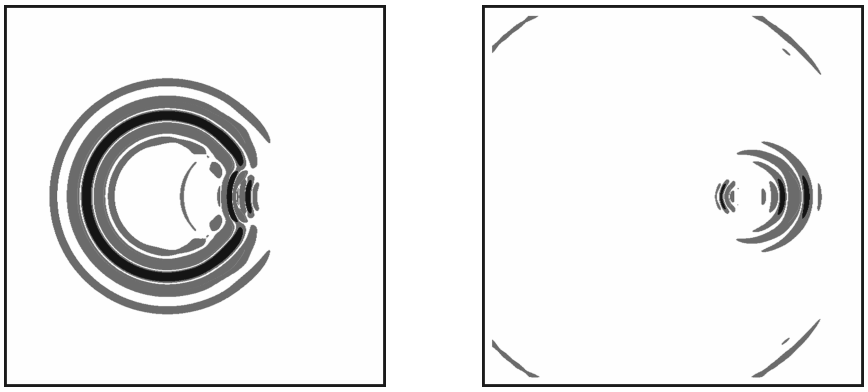

Figure 5. Model 1: Component W, plane Oxy, $t = 1.5$ and 2.7 s

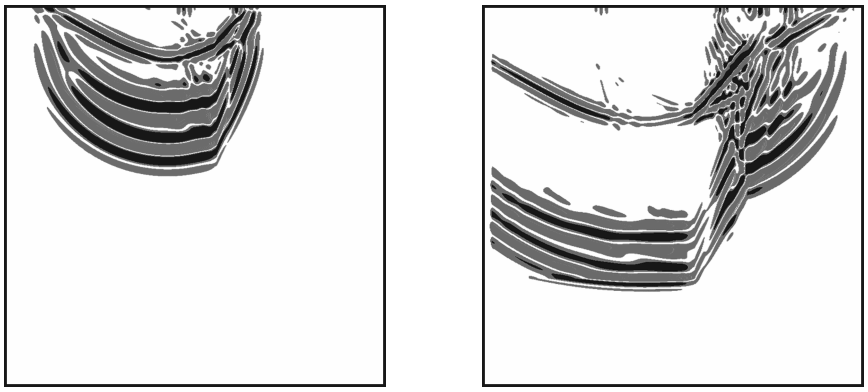

Figure 6. Model 1: Component W, plane Oxz, $t = 1.5$ and 2.7 s

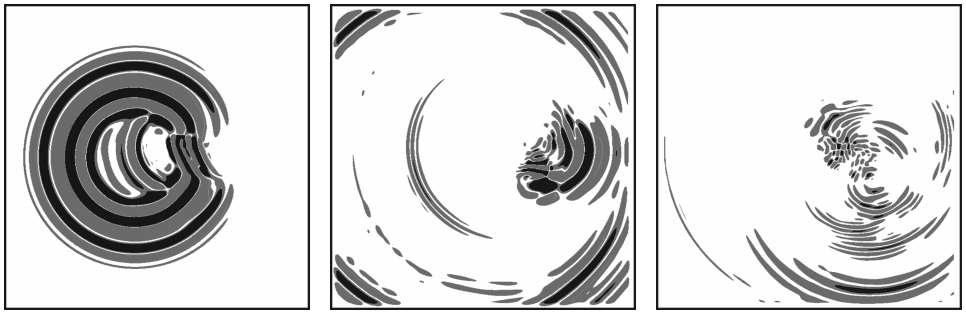

Figure 7. Model 2: Component W, plane Oxy, $t = 1.5$, 2.7, and 4.3 s

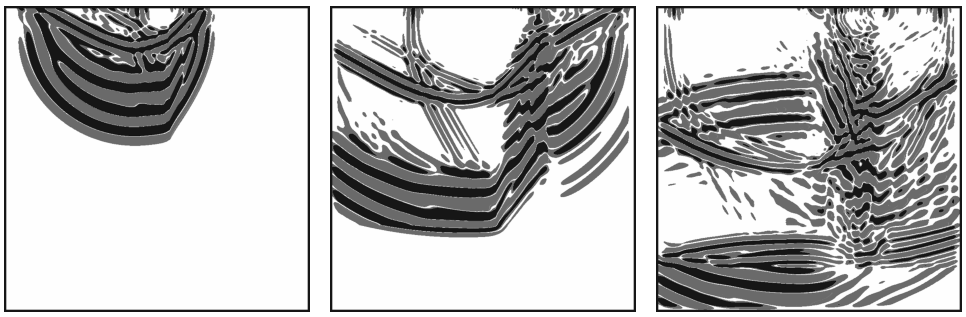

Figure 8. Model 2: Component W, plane Oxz, $t = 1.5$, 2.7, and 4.3 s

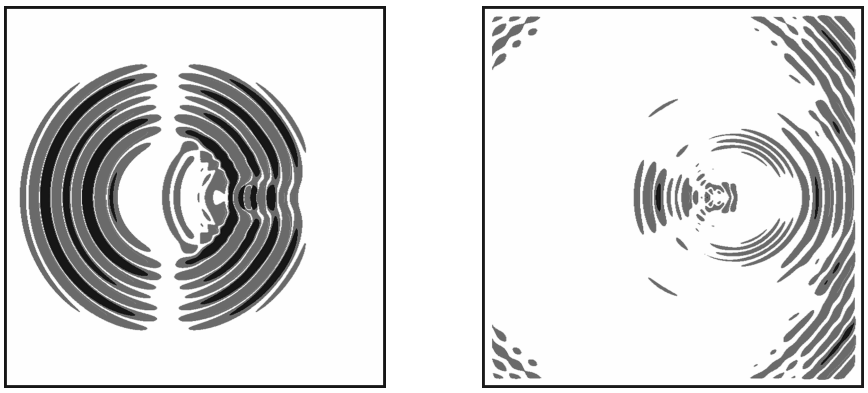

Figure 9. Model 3: Component U, plane Oxy, $t = 1.5$ and 2.7 s

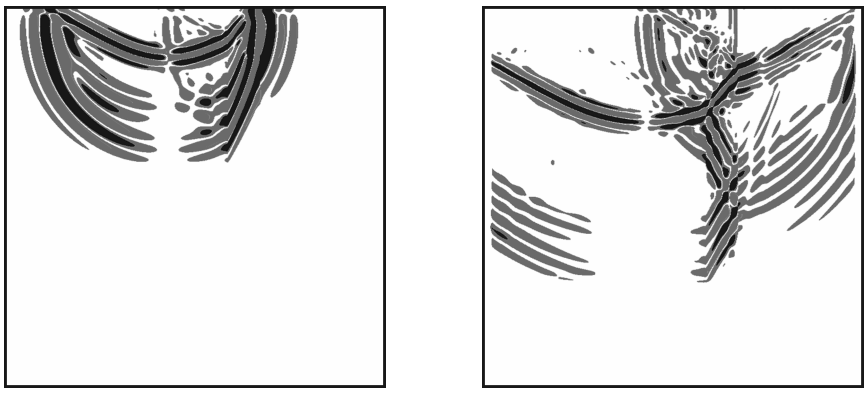

Figure 10. Model 3: Component U, plane Oxz, $t = 1.5$ and 2.7 s

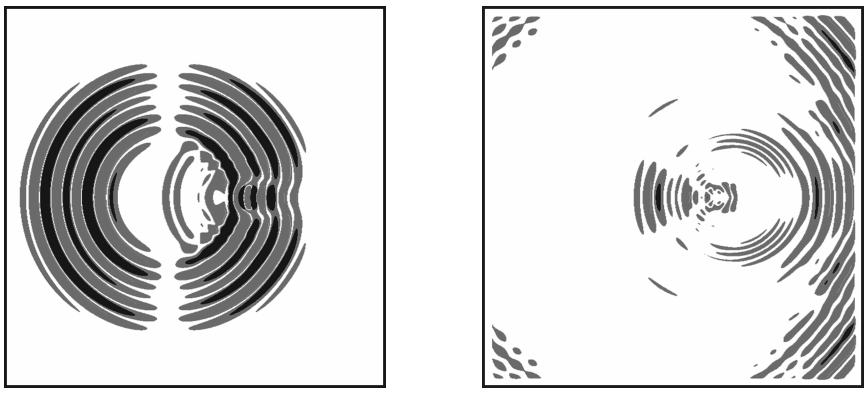

Figure 11. Model 4: Component U, plane Oxy, $t = 4.3$ and 5.1 s

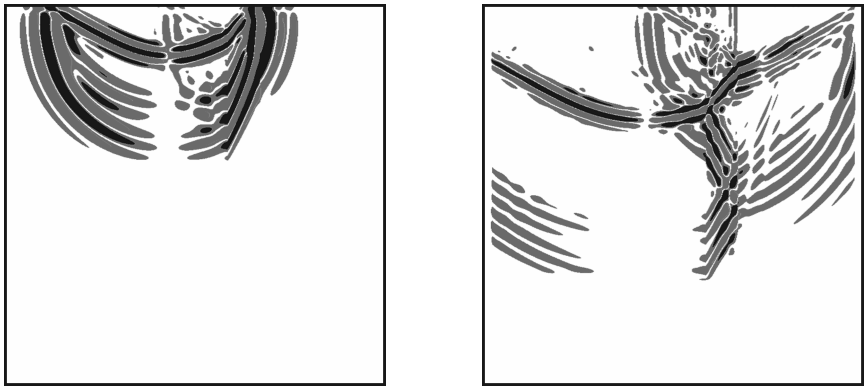

Figure 12. Model 4: Component U, plane Oxz, $t = 4.3$ and 5.1 s

8. Interpretation of the numerical results

In this section, the results obtained with the use of snapshots of a wave field and theoretical seismic traces are discussed. Even for the chosen, simple models of elastic media, we obtain rather a complicated wave picture which is necessary for interpreting. The picture of a wave field can essentially change depending on a set of factors, for example: a distance from a source up to an object, elastic properties of a medium and an object, the sizes of a medium and an object.

In this paper, we do not consider a wave picture which is recorded on the geophones located before object. Therefore we restrict ourselves only to the description of a wave field behind an object.

Several groups of waves (2–9) are distinguished for Model 1 (Figure 13a). Observing the structure of a travel-time curve and with allowance for the arrival time of waves, it is possible to conclude that 2 is PP-wave, 3 is PS-wave, 4 is PPP-wave, 5 is PPS-wave, waves 8–9 are associated with reflection from

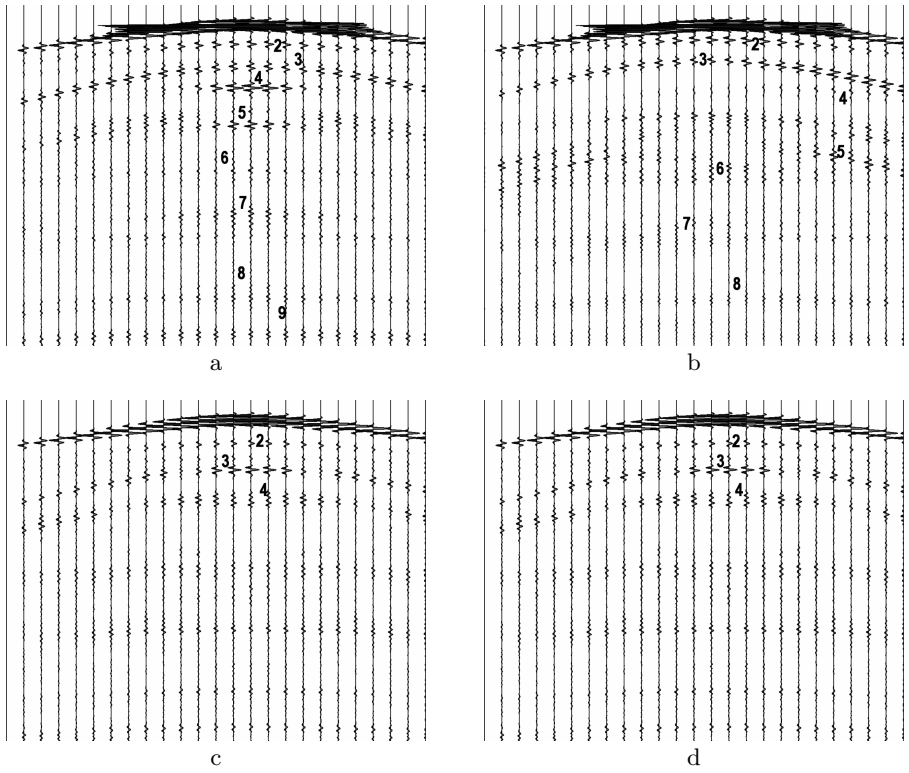

Figure 13. Theoretical seismic traces, "cable" 3, component U: a) Model 1, b) Model 2, c) Model 3, and d) Model 4

the first and the second interfaces. Waves 6 and 7 are generated by the cylinder.

Quite a different picture can be seen in the elliptic cylinder model (Figure 13b). In this case, groups of waves 4 and 5 are absent. Dynamics of PS-wave 3 whose amplitude increases towards the main axis of the elliptic cylinder sharply changes.

For Models 3 and 4 (Figures 13c and 13d), pictures of seismic traces are similar: S-wave is not observed in them. Essentially, the wave picture for waves 2–4 has not changed, while for transverse waves, SS-wave has essentially damped, which is caused by the presence on boundaries of a "cylinder" of heterogeneities comparable with the length of S-wave. This has led to dispersion of energy inside the cylinder.

9. Conclusion

The "toolkit" for carrying out the numerical modeling of elastic waves propagation in models of complex subsurface geometries has been developed. It is

helpful when planning and carrying out natural geophysical studies and interpreting the results obtained.

The numerical modeling calculations on multiprocessor computers are carried out with the help of the developed program. In the future, it is supposed to conduct a series of calculations for various models of media characteristic of the structure of the mud volcano "Karabetov mountain". It is assumed that the obtained numerical results will be used when choosing a scheme and interpreting results of observation with vibroseismic monitoring of this volcano.

References

[1] Glinsky B.M., Sobisevich A.L., Khairetdinov M.S. Experience of the vibroseismic sounding of difficultly constructed geological structures (on an example of mud volcano Shugo) // Proc. Russian Academy of Science. — 2007. — Vol. 413, No. 3. — P. 398–402.

[2] Glinsky B.M., Sobisevich A.L., Fatynov A.G., Khairetdinov M.S. Mathematical simulation and experimental studies of the Shugo mud volcano // J. Volcanology and Seismology. — 2008. — Vol. 2, No. 5. — P. 364–371.

[3] Glinsky B.M., Fatyanov A.G. Numerical-analytical modeling of wave fields in different scale zones of volcanic activity // All-Russia Conference on Calculus Mathematics "CCM-2007", Novosibirsk, June, 18–20, 2007.

[4] Glinsky B.M., Fatyanov A.G. Vibroseismic monitoring of living volcanoes. Active geophysical monitoring of volcanoes // 2nd International Symposium, Novosibirsk, September, 2005. — P. 52–57.

[5] Glinsky B.M., Fatyanov A.G. Studying and monitoring of mud volcanoes with active seismic methods // 2nd International Symposium, Novosibirsk, September, 2005. — P. 52–57.

[6] Mikhailenko B.G. Seismic Fields in Difficultly Constructed Media. — Novosibirsk, 1988.

[7] Bihn M., Weiland T. A stable discretization scheme for the simulation of elastic waves // Proc. 15th IMACS World Congress on Scientific Computation. Modeling and Applied Mathematics (IMACS 1997), August, 1997. — Vol. 2. — P. 75–80.

[8] Collino F., Tsogka C. Application of the pml absorbing layer model to the linear elastodynamic problem in anisotropic heterogeneous media // Geophysics. — 2001. — Vol. 66, No. 1. — P. 294–307.

[9] Komatitsch D., Tromp J. A perfectly matched layer absorbing boundary condition for the second-order seismic wave equation// Geophys. J. Int. — 2003. — Vol. 154. — P. 146–153.

[10] Ilin V.P., Tribis D.Y. Geometrical informatics of continuous media // GraphiCon 2008, Conference Proceedings, Moscow, June 23–27, 2008. — P. 313.